Ionics (2012) 18:267–273
DOI 10.1007/s11581-011-0630-7

ORIGINAL PAPER

A novel PEO-based composite polymer electrolyte with NaAlOSiO molecular sieves powders

De-Jiang Qi · Hong-Qiang Ru · Xiao-Guo Bi · Xiao-Hong Yang · Zi-Ning Ma

Received: 18 March 2011 / Revised: 10 September 2011 / Accepted: 12 September 2011 / Published online: 2 October 2011
© Springer-Verlag 2011

Abstract Ion-conducting thin film polymer electrolytes based on poly(ethylene oxide) (PEO) complexes with NaAlOSiO molecular sieves powders has been prepared by solution casting technique. X-ray diffraction, scanning electron microscopy, differential scanning calorimeter, and alternating current impedance techniques are employed to investigate the effect of NaAlOSiO molecular sieves on the crystallization mechanism of PEO in composite polymer electrolyte. The experimental results show that NaAlOSiO powders have great influence on the growth stage of PEO spherulites. PEO crystallization decrease and the amorphous region that the lithium-ion transport is expanded by adding appropriate NaAlOSiO, which leads to drastic enhancement in the ionic conductivity of the $(PEO)_{16}LiClO_4$ electrolyte. The ionic conductivity of $(PEO)_{16}LiClO_4$-12 wt.% NaAlOSiO achieves $(2.370\pm0.082)\times10^{-4}$ S · cm^{-1} at room temperature (18 °C). Without NaAlOSiO, the ionic conductivity has only $(8.382\pm0.927)\times10^{-6}$ S · cm^{-1}, enhancing 2 orders of magnitude. Compared with inorganic oxide as filler, the addition of NaAlOSiO molecular sieves powders can disperse homogeneously in the electrolyte matrix without forming any crystal phase and the growth stage of PEO spherulites can be hindered more effectively.

Keywords PEO · NaAlOSiO molecular sieves · Ionic conductivity · Polymer electrolyte

D.-J. Qi · X.-H. Yang
Department of Physics, Shenyang Institute of Engineering, Shenyang 110136, People's Republic of China

D.-J. Qi · H.-Q. Ru (✉)
School of Material & Metallurgy, Northeastern University, Shenyang 110004, People's Republic of China
e-mail: hongqiangru@126.com

X.-G. Bi
Department of Energy and Power Engineering, Shenyang Institute of Engineering, Shenyang 110136, People's Republic of China

Z.-N. Ma
Center of test and analysis, China Criminal Police University, Shenyang 110035, People's Republic of China

Introduction

Since Wright's striking discovery that polymer complexes consisting of poly(ethylene oxide) (PEO) and alkali metal salts can exhibit ionic conductivity [1], many different polymer electrolytes and their properties have attracted considerable attention in the past few decades due to several practical applications such as high energy density rechargeable batteries, portable electronics, electric vehicles, and backup power sources in helicopters as well as man-made satellites [2–5]. PEO is often used as matrix material in order that PEO not only has good chemical stability, light weight, good plastic, easy to process, but also can form stable complexes with inorganic salts. Unfortunately, high concentration of crystalline phase presented in PEO/LiX (X=ClO_4^-, BF_4^-, PO_4^-, $CF_3SO_3^-$, etc.) electrolytes system results in a low room temperature ionic conductivity of PEO-based polymer electrolytes. Previous researches show that incorporation of inorganic nanoparticles, propylene carbonate, ethylene carbonate, and polyethylene glycol into the PEO/LiX electrolytes system can improve the ionic conductivity effectively. ZnO [6], ZrO_2 [7], SiO_2 [8–10], MgO [11], CeO_2 [12], Al_2O_3 [13], Sm_2O_3 [14], TiO_2 [15], etc. as an inorganic filler have been deeply studied. MCM-41 [16, 17], ZSM-5 [18–21], SBA-15 [22, 23], and other porous materials are

also helpful to improve the ionic conductivity. In addition, PEO-NaI [24], PEO-KOH [25], PEO-$Mg(NO_3)_2$ [26], PEO-$NaPO_3$ [27], and many other novel PEO-based polymer electrolytes [28–44] have also been extensive investigated. Indeed, in these past years, the limit of PEO crystalline behavior has been overcome by introducing inorganic oxides. But inorganic particles could not dissolve in an organic solvent. Inhomogeneous mixed-phase systems lead to a low ionic conductivity.

In this paper, we report a novel PEO-based composite polymer electrolyte using NaAlOSiO ($Na_{56}[(AlO_2)_{56}(SiO_2)_{136}]$) molecular sieves powders as the filler. As far as we know, this research has not appeared in the other literatures and the properties of such composite polymer electrolyte have not been investigated so far. The molecular weight range of PEO is 1×10^5~1×10^6, depending on the chain length of polymer. Due to the existence of C-O-C chemical bond, PEO matrix can form a stable complex with certain inorganic salts. Different molecular weight of PEO determines different physical properties, including the solubility in organic solvents and mechanical properties. If the molecular weight is too big, the long molecular chain of PEO led to PEO solubility in organic solvents decreasing, which is not conducive to the integration of polymer and filler materials. But if the molecular weight is too small, mechanical properties are poor. In our work, molecular weight M_w=500,000 g/mol of PEO as matrix materials are used. We observed a very large improvement of ion conductivity by addition of these NaAlOSiO molecular sieves powders. The excellent performances of the ion conductivity suggest that the novel $(PEO)_{16}LiClO_4$-NaAlOSiO composite electrolyte can serve as a candidate material for lithium polymer batteries and electrochemical display smart windows.

Experimental

PEO (Shanghai YuKing Chemtech Co., Ltd.) with an average molecular weight of M_w=500,000 g/mol and inorganic salt $LiClO_4$ (Sinopharm Chemical Reagent Co., Ltd. in China) were dried in a vacuum oven for 48 h at 50 °C and 120 °C, respectively, prior to use. NaAlOSiO molecular sieves powders (Nankai University Catalyst Company) were employed as filler. Acetonitrile (Shanghai Chemical Reagent Co., Ltd. in China) was refluxed at a suitable temperature under nitrogen atmosphere prior to use.

The polymer electrolytes were prepared by mixing $LiClO_4$ and PEO with different content of NaAlOSiO molecular sieves powders in acetonitrile solution in proportions corresponding to 16 M units of ethylene oxide (CH_2CH_2O) per lithium-ion (PEO: $LiClO_4$ 16:1) at room temperature. The obtained solution was poured onto a glass dish and the films were dried under vacuum environment slowly in order to get rid of the residue solvent. All the operations and storage were carried out in the vacuum glove box (protective gas is nitrogen). Finally, the electrolyte films of thickness ranging from 100 to 150 μm were formed.

The structural and phase behavior of the conducting polymer electrolyte (CPE) films were studied using X-ray diffraction (XRD) technique. The XRD patterns were recorded at room temperature using Xbd2008aX X-ray diffractometer with Cu-K_α radiation (λ=1.54056 Å), and were performed at 36 KV and 20 mA with a scanning rate of 4°/min. The surface morphologies of the CPEs were investigated using scanning electron microscopy (SEM; HITACHI S-3400N II). Differential scanning calorimeter (DSC) measurements were carried out using a PerkinElmer Pyris-1 calorimeter in temperature range from −70 °C to 100 °C with heating rate of 20 °C/min. The alternating current (AC) impedance measurements of the PEO films were performed using an electrochemical analysis system (Solartron1260A wide frequency response and the 1287A electrochemical interface) in the frequency range of 0.1 Hz~1 MHz. The electrolyte was sandwiched between two stainless steel (SS) blocking electrodes to form a symmetrical SS|electrolyte|SS cell configuration before testing.

Results and discussion

XRD spectra

XRD technique is often performed to identify intercalated structures through Bragg's equation: $\lambda = 2d\sin\theta$, where λ is the wavelength of the X-ray radiation used in the diffraction experiment, d corresponds to the interlayer spacing between diffraction lattice planes and θ is the measured diffraction angle. The XRD spectra of the $(PEO)_{16}LiClO_4$-x wt.% NaAlOSiO (x=0, 8, 15) composites at room temperature are shown in Fig. 1. The two intensive

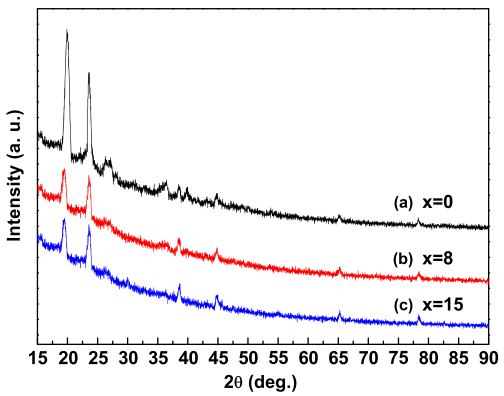

Fig. 1 X-ray diffraction patterns of $(PEO)_{16}LiClO_4$-x wt.% NaAlOSiO (x=0, 8, 15)

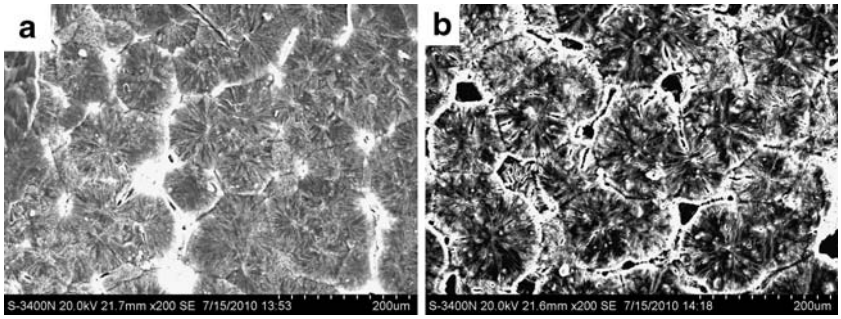

Fig. 2 SEM images of the **a** pure PEO and **b** $(PEO)_{16}LiClO_4$

characteristic diffraction peaks of the crystalline PEO appear at $2\theta=19°$ and 23°. After 8 wt.% NaAlOSiO addition incorporated into the $(PEO)_{16}LiClO_4$ electrolyte matrix, the diffraction peaks of the CPE film become weaker, which indicates a rapid decrease of the PEO crystallinity. With the addition of 15 wt.% NaAlOSiO to the $(PEO)_{16}LiClO_4$ matrix, the intensities of the characteristic peaks retained the same as that of the $(PEO)_{16}LiClO_4$-8 wt.% NaAlOSiO composite. Since no distinct peaks of NaY are observed in host polymer electrolyte, the ionic status of Na^+ and $(AlOSiO)^-$ can been seen. This may lead to an additional conducting species, i.e., Na^+ which may be one reason for enhancement in ionic conductivity. A comparison of XRD spectra shows that the NaAlOSiO has a major influence on the crystallization process of $(PEO)_{16}LiClO_4$ matrix. By introduction of NaAlOSiO, the crystallinity degree of PEO matrix decreases. However, the characteristic peaks remain unchangeable in the CPE films when NaAlOSiO content more than 8 wt.%.

SEM micrographs

The surface morphology of the CPEs samples are presented in Figs. 2 and 3, respectively. It can be seen from Fig. 2 that pure PEO and $(PEO)_{16}LiClO_4$ show a typical crystal morphology with spherical shape structure. The spherulites crystal distribution is compact and ordered. Compared with pure PEO, $(PEO)_{16}LiClO_4$ pattern's spherulites crystal are larger, but the number is fewer. After different amount of NaAlOSiO particles were incorporated in the $(PEO)_{16}LiClO_4$ electrolyte matrix, drastic changes of surface morphology appear in Fig. 3. With the increase of NaAlOSiO content (less than 12 wt.% NaAlOSiO), the surface morphology of CPEs are changed drastically. A dramatic improvement from branch shape to crosslinked network was observed. Crystallization kinetics of PEO matrix is related to the ordered helical structure formed by the molecular self-assembly without any external factor. PEO polymer exists the structure of elementary nucleus. The

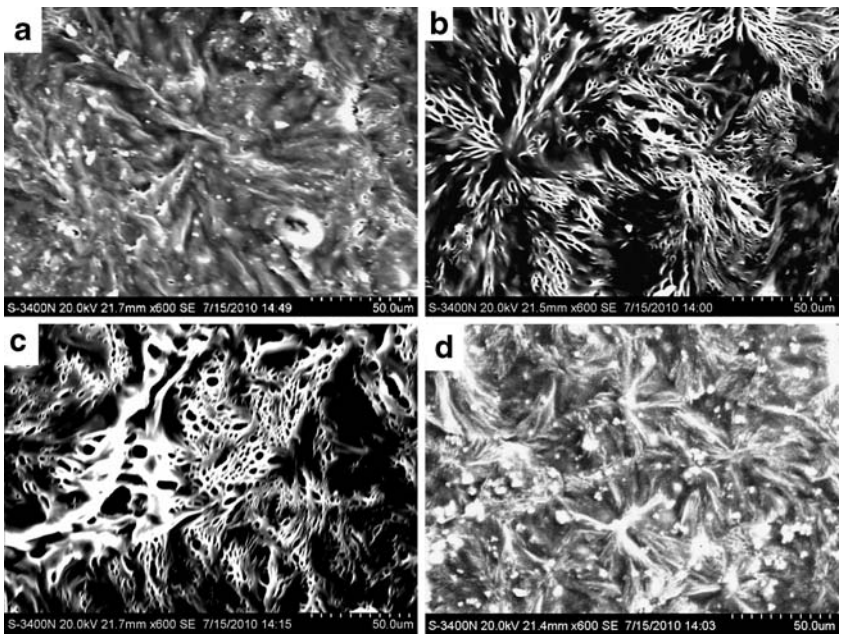

Fig. 3 SEM images of the $(PEO)_{16}LiClO_4$-x wt.% NaAlOSiO: **a** $x=5$, **b** $x=8$, **c** $x=12$, **d** $x=20$

Table 1 Thermodynamic properties of composite polymer electrolytes from DSC analysis (initial test day)

Sample	Glass point, t_g/°C	Melting point, t_m/°C	Melting enthalpy, ΔH_m/J · g^{-1}	Crystallinity, X_c/%	Crystallinity X_x/%[a]
$(PEO)_{16}LiClO_4$	−36.72	55.71	118.45	55.43	64.76
$(PEO)_{16}LiClO_4$-5 wt.% NaAlOSiO	−39.42	53.86	79.05	36.99	–
$(PEO)_{16}LiClO_4$-8 wt.% NaAlOSiO	−41.76	52.33	74.93	35.06	38.17
$(PEO)_{16}LiClO_4$-12 wt.% NaAlOSiO	−43.21	51.60	65. 80	30.79	–
$(PEO)_{16}LiClO_4$-15 wt.% NaAlOSiO	−45.09	49.45	59.84	28.00	35.56
$(PEO)_{16}LiClO_4$-20 wt.% NaAlOSiO	−49.53	47.07	63.43	29.68	–

[a]Crystallinity X_x are calculated by XRD data

more ordered of the molecular arrangement, the stronger their crystallization ability. After incorporating NaAlOSiO particles, the molecular chain scission occurs due to the disorder of molecular chain. Thus, the crystalline of PEO tends to become difficult, and the continuous amorphous region is expanded. However, severe aggregated phases and separated phase domains can be detected when NaAlOSiO particle content reaches 20 wt.%. This is because much more NaAlOSiO particles cannot be dispersed homogeneously in the $(PEO)_{16}LiClO_4$ matrix, which leads to accumulation effect that hinder lithium-ion transport (Fig. 3d). The reported effect by [45] of NaY molecular sieve on the composite polymer electrolyte (PVDF-HFP as matrix material) in lithium-ion batteries and the compact structure without any pores was observed and was needed to be addressed. The differences may be attributed to the different structure of matrix material in polymer electrolyte.

Differential scanning calorimetry

The glass transition temperature (t_g), melting temperature (t_m), change of melting enthalpy (ΔH_m), and percentage of crystalline (X_C) of CPE samples are listed in Table 1. The relative percentage of crystalline PEO, X_C, can be calculated with the equation $X_C = \Delta H_m/\Delta H^*$ [46], where ΔH^*=213.7 J · g^{-1} is the melting enthalpy of a completely crystalline PEO sample. With the addition of NaAlOSiO powders, the t_g, t_m, and crystallization behavior of PEO are completely different. The Lewis acid-based interaction between the ether O atoms of PEO and Lewis acid sites on the surface of NaAlOSiO results in decreasing of t_g, t_m, and X_C. The crosslinked network structure of NaAlOSiO powders may provide more Lewis acid sites to interact with the ether O atoms as Lewis base of PEO chains. The low glass transition temperature t_g is important for us to obtain a good flexibility of the polymer chains which are related to the ion transport. The addition of NaAlOSiO powders reduces the X_C, also suggesting that the amorphous phase is enhanced predominantly.

The relationship between crystalline of CPE and time is shown in Fig. 4. The $(PEO)_{16}LiClO_4$ samples have high crystalline, and increase obviously with time, the crystalline of $(PEO)_{16}LiClO_4$ is 55.43% with the initial test day. After 80 days, it achieves 73.85%, increasing nearly 20%. By introducing 5 wt.% NaAlOSiO filler, crystalline increase rapidly within 3 days, but the degree of crystalline is almost unchangeable from the third day to the 80th day. Mixed with 12 wt.% NaAlOSiO filler, the curve is parallel with the former, but has a lower degree of crystalline. When

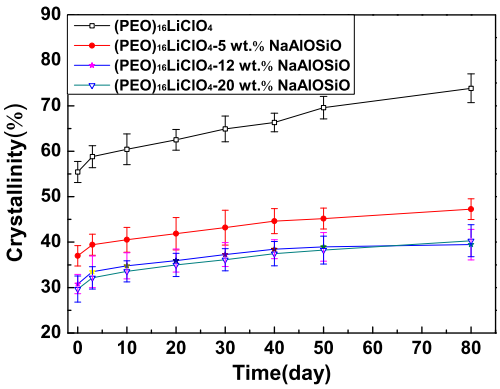

Fig. 4 The relationship between crystallinity and time

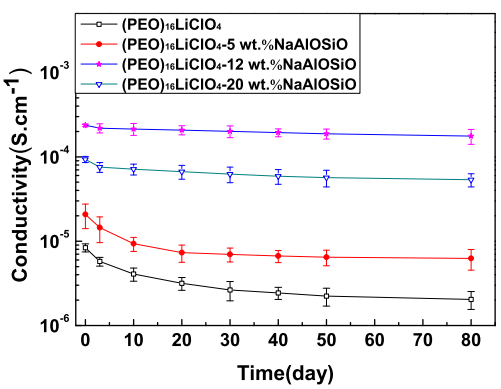

Fig. 5 The relationship between conductivity and time

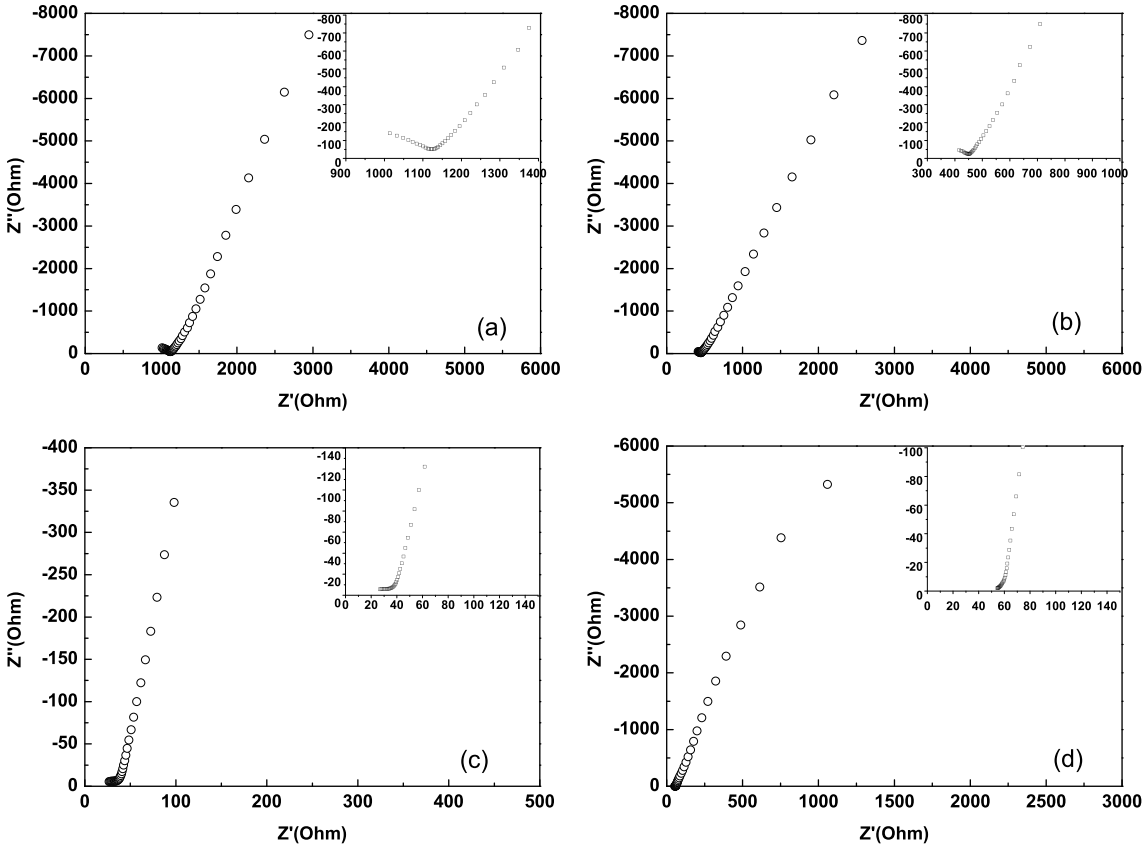

Fig. 6 Room temperature impedance plots for the $(PEO)_{16}LiClO_4$-*x* wt.% NaAlOSiO: **a** *x*=0, **b** *x*=5, **c** *x*=12, **d** *x*=15

NaAlOSiO content is 20 wt.%, the crystalline of CPEs decrease with little range. Figure 5 displays the time evolution of ionic conductivity. The enhancement in ionic conductivity based on the decrease in crystallinity with addition of filler NaAlOSiO is supported. $(PEO)_{16}LiClO_4$-12 wt.% NaAlOSiO shows initial ionic conductivity of nearly two magnitudes higher than that of $(PEO)_{16}LiClO_4$, and only a small decreasing of ionic conductivity within 80 days.

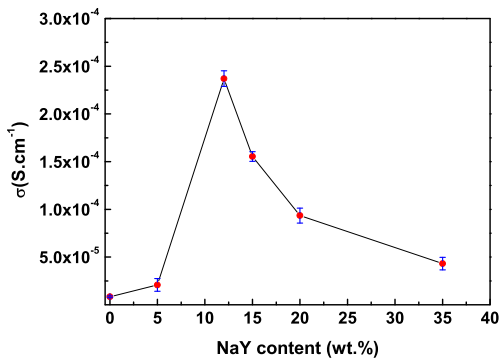

Fig. 7 The ionic conductivity of CPEs at room temperature (18 °C) with different NaAlOSiO content

Impedance spectroscopy and ionic conductivity

Ionic conductivity of the CPE film is determined by AC impedance spectroscopy. The conductivity value σ is calculated from the equation $\sigma = d/(R_b S)$, where *d* is the thickness and *S* is the area of the sample, and R_b is the bulk resistance, which is determined from the impedance spectra or equivalent circuit. Figure 6 displays impedance spectra of $(PEO)_{16}LiClO_4$-*x* wt.% NaAlOSiO. It can be seen from Fig. 6c that intercept of the high frequency arc on the real axis is seen to decrease. Thus, the ionic conductivity is to increase with the temperature increases. A minimum value of the bulk resistance R_b appears in addition to 12 wt.%

Table 2 Ionic conductivity from different CPE systems at room temperature

CPEs	Ionic conductivity ($S \cdot cm^{-1}$)
PEO-$LiClO_4$-5 wt.% TiO_2 (10 nm) [47]	1.40×10^{-4}
PEO-LiClO4-25 wt.% Al_2O_3 [48]	1.0×10^{-6}
PEO-LiClO4-10 wt.% Sm_2O_3 [14]	4.45×10^{-5}
PEO-LIBETI-10 wt.% SiO2 [10]	1.5×10^{-5}

NaAlOSiO. The ionic conductivity at 18 °C with different content of addition NaAlOSiO is shown in Fig. 7. With the NaAlOSiO content increases, the ionic conductivity is increasing accordingly. The ionic conductivity achieve maximum value $(2.370\pm0.082)\times10^{-4}$ S · cm^{-1} with the addition of 12 wt.% NaAlOSiO, enhancing two orders of magnitude compared with $(PEO)_{16}LiClO_4$ system. It is very close to the standards of application. Compared with other inorganic nanoparticles as inert filler, the addition of NaAlOSiO increases the ionic conductivity of the $(PEO)_{16}LiClO_4$ more noticeably and remarkably as shown in Table 2. This may be the reason that the appropriate amount of NaAlOSiO powders can provide more Lewis acid sites to interact with the ether O atoms of PEO chains, which lead to the better conductivity compared to some inorganic particles. Without NaAlOSiO, the ionic conductivity has only $(8.382\pm0.927)\times10^{-6}$ S · cm^{-1}. However, when NaAlOSiO content exceeds 12 wt.%, the ionic conductivity begin to decline. This is because the excessive NaAlOSiO powders were accumulated, which hindered lithium-ion transport.

Conclusion

In summary, a novel all solid-state composite polymer electrolyte $(PEO)_{16}LiClO_4$-*x* wt.% NaAlOSiO (*x*=0, 5, 8, 12, 15, 20, 35) has been prepared by solution casting technique for the first time. XRD, SEM, DSC technology, and AC impedance method were employed to investigate the effect of NaAlOSiO addition on the $(PEO)_{16}LiClO_4$ electrolyte matrix. Experimental results showed that NaAlOSiO has great influence on the growth stage of PEO spherulites. Through adding appropriate NaAlOSiO, the molecular chain scission occurs due to the disorder of molecular chain. Thus, PEO crystallization decrease and the amorphous region of the lithium-ion transport are expanded. However, severe aggregated phases and separated phase domains can be detected when NaAlOSiO pargicles content reaches 20 wt.%. The high ionic conductivity $(2.370\pm0.082)\times10^{-4}$ S · cm^{-1} achieve at room temperature with the addition of 12 wt.% NaAlOSiO was observed. Compared with the sample without NaAlOSiO molecular sieves powders, there is an increase of two orders of magnitude.

Acknowledgments This work was supported in part by the Natural Science Foundation of Liaoning Province (grant no. 20060587) and Natural Science Foundation of Shenyang (grant no. 1032044-1-02).

References

1. Fenton DE, Parker JM, Wright PV (1973) Polymer 14:589
2. Croce F, Appetecchi GB, Persi L, Scrosati B (1998) Nature 394:456
3. Yang YWC, Wang YL, Chen YT, Li YK, Chen HC, Chiu HY (2008) J Power Sources 182:340
4. Dey A, Karan S, De SK (2008) Solid State Ionics 178:1963
5. Zhang H, Maitra P, Wunder SL (2008) Solid State Ionics 178:1975
6. Dang ZM, Fan LZ, Zhao SJ, Nan CW (2003) Mater Res Bull 38:499
7. Croce F, Sacchetti S, Scrosati B (2006) J Power Sources 161:560
8. Fan LZ, Nan CW, Zhao SJ (2003) Solid State Ionics 164:81
9. Fan LZ, Nan CW, Li M (2003) Chem Phys Lett 369:698
10. Kim JW, Ji KS, Lee JP, Park JW (2003) J Power Sources 119–121:415
11. Kumar B, Scanlon L, Marsh R, Mason R, Higgins R, Baldwin R (2001) Electrochim Acta 46:1515
12. Dey A, Karan S, De SK (2010) J Phys Chem Solids 71:329
13. Köster TK-J, Wullen L (2010) Solid State Ionics 181:489
14. Chu PP, Reddy MJ (2003) J Power Sources 115:288
15. Liu Y, Lee JY, Hong L (2003) J Appl Polym Sci 89:2815
16. Hu LF, Tang ZL, Zhang ZT (2007) J Power Sources 166:226
17. Kao HM, Tsai YY, Chao SW (2005) Solid State Ionics 176:1261
18. Xi J, Miao S, Tang X (2004) Macromolecules 37:8592
19. Xi J, Ma X, Cui M, Huang X, Zheng Z, Tang X (2004) Chin Sci Bull 49:785
20. Xi J, Tang X (2004) Chem Phys Lett 393:271
21. Xi J, Qiu X, Cui MZ, Tang X, Zhu WT, Chen LQ (2006) J Power Sources 156:581
22. Reddy MJ, Chu PP (2004) J Power Sources 135:1
23. Reddy CS, Wu GP, Zhao CX, Zhu QY, Chen W, Kalluru RR (2007) J Non-Cryst Solids 353:440
24. Zon A, Mos B, Verkerk P, Leeuw SW (2001) Electrochim Acta 46:1717
25. Mohamad AA, Haliman H, Sulaiman MA, Yahya MZA, Ali A (2008) Ionics 14:59
26. Ramalingaiah S, Srinivas RD, Jaipal RM, Laxminarsaiah E, Subba RU (1996) Mater Lett 29:285
27. Bhide A, Hariharan K (2006) J Power Sources 159:1450
28. Mohan VM, Raja V, Sharma AK, Narasimha RVVR (2006) Ionics 12:219
29. Rajendran S, Bama VS, Prabhu MR (2010) Ionics 16:27
30. Bandara TMWJ, DissaNayake MAKL, Ileperuma OA, Varaprathan K, Vignarooban K, Mellander BE (2008) J Solid State Electrochem 12:913
31. Mohamad SA, Ali MH, Yahya R, Ibrahim ZA, Arof AK (2007) Ionics 13:235
32. Vickraman P, Aravindan V, Lee Y-S (2010) Ionics 16:263
33. Zhang J, Huang X, Fu J, Huang Y, Liu W, Tang X (2010) Mater Chem Phys 121:511
34. Praveen D, Bhat SV, Damle R (2011) Ionics 17:21
35. Derrien G, Hassoun J, Sacchetti S, Panero S (2009) Solid State Ionics 180:1267
36. Wanga YJ, Pana Y, Wanga L, Panga MJ, Chen L (2005) Mater Lett 59:3021
37. Ramesh S, Chao LZ (2011) Ionics 17:29
38. Barbosa PC, Rodrigues LC, Silva MM, Smith MJ, Parola AJ, Pina F, Pinheiro C (2010) Electrochim Acta 55:1495
39. Johan MR, Fen LB (2010) Ionics 16:335

40. Chandrasekaran R, Sathiyamoorthi R, Selladurai S (2009) Ionics 15:703
41. Gnedenkov SV, Khrisanfova OA, Zavidnaya AG, Sinebryukhov SL, Egorkin VS, Nistratova MV, Yerokhin A, Matthews A (2010) Surf Coat Technol 204:2316
42. Pradhan DK, Samantaray BK, Choudhary RNP, Karan NK, Thomas R et al (2011) Ionics 17:127
43. Thakur AK (2011) Ionics 17:109
44. Rajendran S, Babu R, Sivakumar P (2008) J Membr Sci 315:67
45. Jiang YX, Chen ZF, Zhang QC, Xu JM, Dong QF, Huang L, Sun SG (2006) J Power Sources 160:1320
46. Li X, Hsu SL (1984) J Polym Sci Polym Phys Ed 221:331
47. Lin CW, Hung CL, Venkateswarlu M et al (2005) J Power Sources 146:397
48. Gu NY, Qian XM, Chen ZL, Jiang JG, Yang XR, Dong SJ (2001) Chem J Chin Univ 22:403